Supplementary Information

Self-Assembly of Cyclic Peptide Monolayers by Hydrophobic Supramolecular Hinges

Ignacio Insua[1,2], Annalisa Cardellini[3,4], Sandra Díaz[1], Julian Bergueiro[1], Riccardo Capelli[5], Giovanni M. Pavan[3,4*], Javier Montenegro[1*]

[1] Centro Singular de Investigación en Química Biolóxica e Materiais Moleculares (CIQUS), Departamento de Química Orgánica, Universidade de Santiago de Compostela, 15705, Spain.
[2] I+D Farma group (GI-1645). Departamento de Farmacoloxía, Farmacia e Tecnoloxía Farmacéutica. Facultade de Farmacia, Universidade de Santiago de Compostela, 15782, Spain.
[3] Department of Applied Science and Technology, Politecnico di Torino, 10129 Torino, Italy.
[4] Department of Innovative Technologies, University of Applied Sciences and Arts of Southern Switzerland, Polo Universitario Lugano, 6962 Lugano-Viganello, Switzerland.
[5] Department of Biosciences, University of Milan, 20133 Milano, Italy.

* Email: giovanni.pavan@polito.it; * Email: javier.montenegro@usc.es.

Contents:

1. Abbreviations

ACN: acetonitrile, AFM: atomic force microscopy, All: allyl, CD: Circular Dichroism, CP: cyclic peptide, Boc: *tert*-butyloxycarbonyl, DCM: dichloromethane, DIC: *N,N'*-diisopropylcarbodiimide, DIPEA: *N,N*-diisopropylethylamine, DMAP: 4,dimethylaminopyridine, DMF: *N,N*-dimethylformamide, ESI: electrospray ionisation, Fmoc: 9-fluorenylmethoxycarbonyl, Glu: glutamic acid, His: histidine, HOBt: hydroxybenzotriazole, HR-MS: high resolution mass spectrometry, HPLC-MS: high performance liquid chromatography-mass spectrometry, Leu: leucine, HBTU: *N,N,N',N'*-tetramethyl-*O*-(1*H*-benzotriazol-1-yl)uronium hexafluorophosphate, NMR: nuclear magnetic resonance spectroscopy, OAc: acetate, Ph: phenyl, PyAOP: (7-azabenzotriazol-1-yloxy) tripyrrolidinophosphonium hexafluorophosphate, SPPS: solid phase peptide synthesis, STEM: scanning transmission electron microscopy, ^{t}Bu: tert-butyl, TFA: trifluoroacetic acid, THF: tetrahydrofuran ThT: thioflavin T, TIPS: triisopropylsilane, Trp: tryptophan, Trt: Trityl.

2. Materials

Chemical reagents were acquired from Acros Organics, Aldrich, Carbolution, Fisher Scientific, Iris Biotech, and Novabiochem without additional purification unless otherwise specified. All solvents employed were HPLC grade or synthesis grade, except dry CH_2Cl_2 which was dried under reflux over CaH_2. D_2O was purchased from EMD Millipore. Glass slides for fluorescence microscopy were obtained from Ibidi (Cat# 80827). TEM grids (Cu carbon type-B, 300 mesh) and PELCO® mica discs for AFM were acquired from Ted Pella.

Nuclear Magnetic Resonance (NMR) spectra were recorded on a Varian 500 MHz spectrometer. Chemical shifts are reported in ppm (δ) referenced to D_2O (4.79) or CD_3OD (3.31) residual signal. Spin multiplicities are reported as a singlet (s), doublet (d), with coupling constants (*J*) given in Hz, or multiplet (m). High-performance liquid chromatography coupled with mass spectrometry (HPLC-MS) analyses were carried out on an Agilent 1260 Infinity II connected to a 6120 Quadrupole MS detector using an Agilent SB-C18 column with *Solvent A:Solvent B* gradients between 5:95 (*Solvent A*: H_2O with 0.1% TFA; *Solvent B*: CH_3CN with 0.1% ACN. High-resolution mass (HR-MS) determination using ESI-MS was acquired in a Bruker MicroTOF mass spectrometer. Data are expressed in units of mass per unit of load (m/z). Fourier-transform infrared spectroscopy (FT-IR) measurements were performed on a Perkin Elmer Spectrum Two. Circular dichroism spectra were acquired on a Jasco J-1100 CD spectrometer equipped with temperature control. Epifluorescence micrographs were taken with a Nikon Eclipse T*i* (60x immersion objective, Excitation=475/35 nm; Emission=530/43 nm). Scanning transmission electron microscopy (STEM) images were acquired on a FESEM Ultra plus (Zeiss) operating at 20 kV. AFM analysis was carried out on a NX-10 microscope in non-contact mode and using ACTA 10M cantilevers (Park Systems).

3. Peptide synthesis

All peptides were synthesised manually following the standard Fmoc solid phase peptide protocol described by our group.[1]

Wang resin (100 mg; loading 1.0 mmol/g) was soaked in dry DMF (4 mL) for 30 min. The solvent was filtered off, and a solution of Fmoc-D-Glu-OAll (163.7 mg, 0.4 mmol) in dry DMF (2 mL) was stirred at rt for 5 min, then a solution of HOBt (54 mg, 0.4 mmol) and DIC (62 μL, 0.4 mmol) in dry THF (2 mL) and a solution of DMAP (12.2 mg, 0.1 mmol) in dry THF (2 mL) were successively added. The suspension was mechanically shaken (3-4h) and then, the resin was washed with DMF (3 x 4 mL x 1 min) and DCM (3 x 4 mL x 1 min) under a nitrogen stream. A mixture of acetic anhydride and pyridine (1:1, 4mL) was added to the reaction vessel and left to react for 30 min under a nitrogen stream to end cap any unreacted hydroxyl groups on the resin. Finally, was washed with DCM (3 x 4mL x 1 min) and vacuum dried to obtain the desired Fmoc-D-Glu-(Wang Resin)-OAll. The loading resin was calculated using Fmoc test to get mmol/g [2]. For this, a small portion of the resin (*ca* 5 mg) was treated with a solution of piperidine in DMF (20% v/v, 4 mL) for 30 min. After this time, the concentration of dibenzofulvene-piperidine adduct from the Fmoc removal was measured by averaging its absorbance at 290 and 301 nm of a small aliquot (20 μL).

All reagent amounts were calculated based on the loading calculated above. Subsequent coupling cycles consisted of Fmoc removal upon treatment with piperidine in DMF (20% v/v, 4 mL) for 15 min and coupling protocol using a solution of (D or L)-α-amino acids (4 equiv), *N*-HBTU (3.8 equiv), DIPEA (6 equiv) in DMF (4 mL) under a nitrogen stream for 30 min. Washings with DMF (3 x 4 mL x 1 min) were performed after each step. Having coupled the last amino acid, the resin was washed with DCM (4 mL x 1 min) and filtered.

For the deprotection of the *C*-terminal group (allyl) a solution of PPh_3 (34.4 mg, 0.13 mmol), *N*-methylmorpholine (95 μL, 0.87 mmol), phenylsilane (107 μL, 0.87 mmol) and $Pd(OAc)_2$ (5.8 mg, 0.026 mmol) in dry DCM (4 mL) was added to the resin and mechanically shaken for 3 h. The resin was washed with DCM (3 x 4 mL x 1 min) and then filtered with a solution of DIPEA in DMF (2% v/v, 4 mL). Finally, was soaked in a solution of sodium diethyldithiocarbamate (0.5% w/v in DMF, 2 x 4 mL x 30 min) to remove all traces of Pd.

For the deprotection of the *N*-terminal group (Fmoc) the resin was treated with a solution of piperidine in DMF (20% v/v, 4 mL) for 30 min. After filtration, the resin was washed with DMF (3 x 4 mL x 1 min), a solution of DIPEA in DMF (2 % v/v, 4 mL) was passed through the resin filtering it and finally was washed with a solution of LiCl in DMF (0.5% v/v, 4 mL, 15 min).

Cyclisation was carried out by reacting a solution of PyAOP (177.3 mg, 0.34 mmol) and DIPEA (90 μL, 0.36 mmol) in DMF (4 mL) for 2 h by mechanical stirrer. After washing with DMF (3 x 4 mL x 1 min) and DCM (3 x 4 mL x 1 min), the cyclisation was repeated twice more in the same conditions.

The peptide was cleaved from the resin by the addition of a freshly prepared TFA cocktail (4 mL, TFA:DCM:H_2O:TIPS, 90:5:2.5:2.5), this mixture was shaken for 2 h and then filtered. The resin was washed with TFA (0.5 mL) twice and concentrated under nitrogen. The concentrated reaction crude was precipitated dropwise into 40 mL of cold diethyl ether. The resulting suspension was centrifuged and the pellet was then dissolved in a 1:1 mixture of MilliQ H_2O:ACN and purified by semipreparative HPLC using a Phenomenex Luna C18 100Å column. Solvents used were H_2O + 0.1%v/v TFA (solvent A) and CH_3CN + 0.1%v/v TFA (solvent B) and the method used a gradient of H_2O + 0.1% TFA: CH_3CN + 0.1% TFA → 95:5 (0 min) to 25:75 (30 min). Peptide fractions were concentrated *in vacuo* to remove ACN and TFA and the remaining solution was freeze-dried. A white powder was obtained for all cyclic peptides.

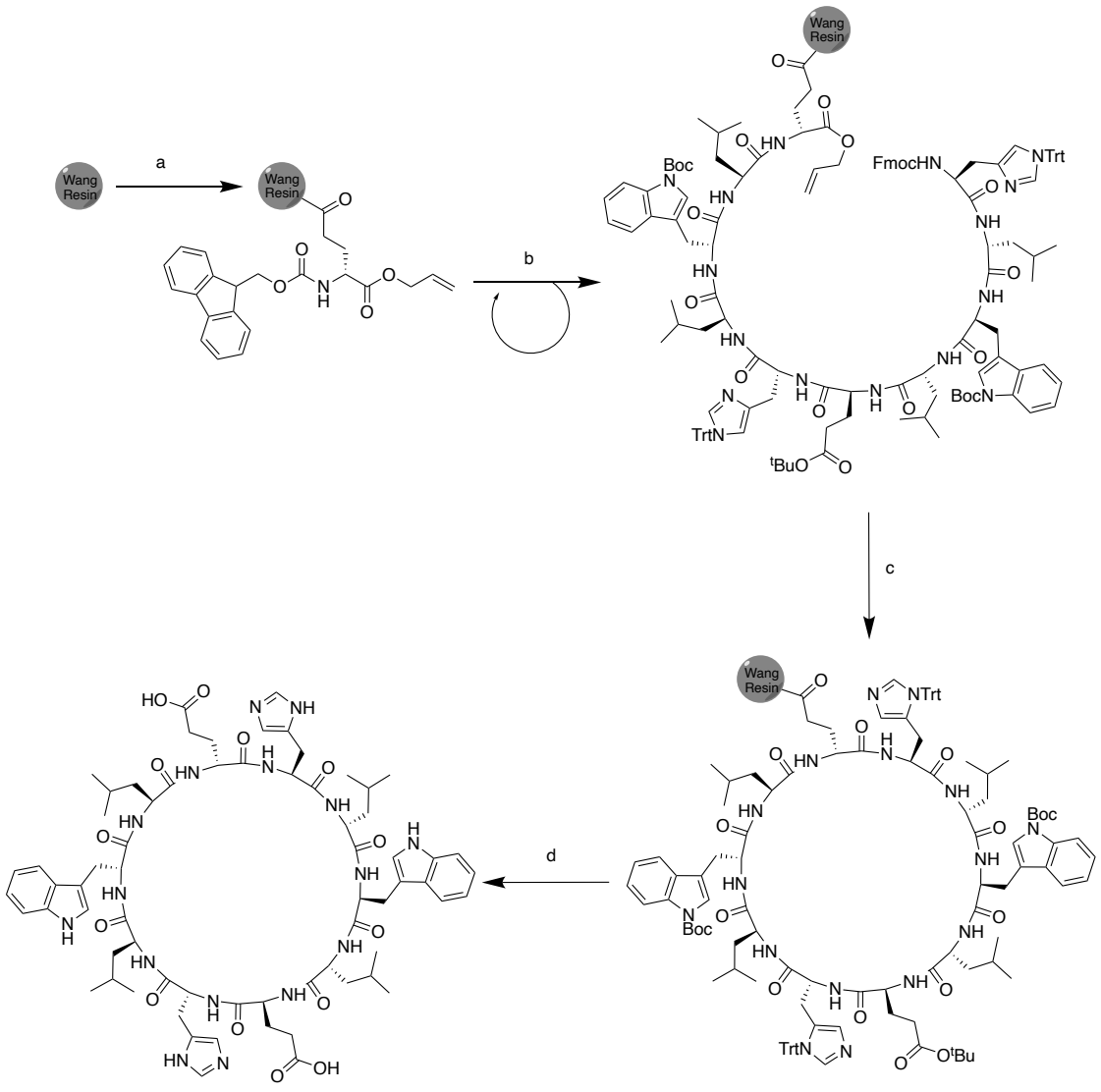

Solid-Phase Peptide Synthesis Scheme. *a) Wang resin functionalisation: Fmoc-D-Glu-OAll in DMF, HOBt, DIC, DMAP in THF, 3h. b) Peptide elongation: i) Piperidine 20% v/v in DMF, 15 min; ii) Fmoc-amino acid, N-HBTU, DIPEA, DMF, 30 min. (repeat 9 cycles). c) i) OAll removal: Palladium (II) acetate, triphenylphosphine, phenylsilane, 4-methylmorpholine, DCM, 3h; ii) Fmoc removal: piperidine 20% v/v in DMF, 30 min; iii) Peptide cyclisation: PyAOP, DIPEA, DMF, 2h (repeat twice). d) Peptide cleavage: TFA-DCM-H_2O-TIPS (90:5:2.5:2.5), 2h.*

4. Peptide characterisation

CP10: Yield = 26 mg (19%). HPLC-MS (C18-ESI, +eV, gradient of H_2O + 0.1% TFA: CH_3CN + 0.1% TFA → 95:5 (0 min) to 5:95 (12 min) R_t = 8.6 min; m/z = 1357.6 ($[M+H]^+$), 679.6 ($[M+2H]^{2+}$). HRMS (ESI, +eV, m/z) Calculated for $C_{68}H_{93}N_{16}O_{14}$ ($[M+H]^+$): 1357.68; found: 1357.7050. ^{1}H-NMR (500 MHz, CD_3OD) δ (ppm): 0.43-0.52 (m, 5H, Leu), 0.59-0.66 (m, 5H, Leu), 0.8-0.92 (m, 14H, Leu), 1.2-1.5 (m, 12H, Leu), 2.0-2.5 (m, 8H, Glu -CH_2-), 2.9-3.2 (m, 8H, His -CH_2-, Trp -CH_2-), 3.9-5.3 (m, 10H, H_α), 6.9-7.03 (m, 2H, Trp -CH=), 7.04-7.1 (m, 4H, Trp -CH=), 7.15-7.2 (s, 1H, His -CH=), 7.2-7.3 (s, 1H, His -CH=), 7.3-7.35 (dd, 2H, $J_{h,h}$ = 8.17, 3.23 Hz, Trp -CH=), 7.5-7.55 (dd, 2H, $J_{h,h}$ = 7.44, 2.99 Hz, Trp -CH=), 8.75-8.77 (s, 1H, His -CH=), 8.8-8.83 (s, 1H, His -CH=).

3L: Yield = 18 mg (15%). HPLC-MS (C18-ESI, +eV, gradient of H_2O + 0.1% TFA: CH_3CN + 0.1% TFA → 95:5 (5 min) to 5:95 (12 min) R_t = 8.6 min; m/z = 1211.7 ($[M+H]^+$), 606.45 ($[M+2H]^{2+}$). HRMS (ESI, +eV, m/z) Calculated for $C_{58}H_{94}N_{14}O_{14}$ ($[M+H]^+$): 1211.71; found: 1211.7134 . ^{1}H-NMR (500 MHz, D_2O) δ (ppm): 0.79-0.99 (m, 37H, Leu), 1.5-1.7 (m, 17H, Leu), 1.8-2.2 (m, 4H, Glu -CH_2-), 2.2-2.4 (m, 4H, Glu, -CH_2-), 3.1- 3.4 (m, 4H, His -CH_2-), 4.3-4.4 (m, 7H, H_α), 4.6-4.7 (m, 3H, H_α), 7.3-7.4 (s, 2H, His -CH=), 8.7-8.8 (s, 2H, His -CH=).

LW: Yield = 22 mg (16%). HPLC-MS (C18-ESI, +eV, gradient of H_2O + 0.1% TFA: CH_3CN + 0.1% TFA → 95:5 (0 min) to 5:95 (20 min) R_t = 11.9 min; m/z = 699.4 ($[M+2H]^{2+}$), 466.8 ($[M+3H]^{3+}$). HRMS (ESI, +eV, m/z) Calculated for $C_{67}H_{84}N_{18}O_{16}$ ($[M+H]^+$): 1396.63; found: 1397.6352 . ^{1}H-NMR (500 MHz, D_2O) δ (ppm): 0.58-0.65 (m, 9H, Leu), 0.70-0.73 (m, 2H, Leu), 1.2-1.3 (m, 2H, Leu), 1.3-1.4 (m, 2H, Leu), 1.7-2.3 (m, 12H, Glu -CH_2-), 2.9-3.3 (m, 10H, His -CH_2-, Trp -CH_2-, overlapped), 4.0-4.7 (m, 10H, H_α, overlapped with solvent signal), 6.8-6.9 (s, 1H, His -CH=), 7.0-7.1 (d, 2H, $J_{h,h}$ = 7.07 Hz Trp -CH=), 7.1-7.3 (m, 4H, Trp -CH= overlapped with 2H, His -CH=), 7.4-7.5 (d, 1H, $J_{h,h}$ = 7.46 Hz, Trp =CH_2=), 7.5-7.55 (d, 1H, $J_{h,h}$ = 7.52 Hz, Trp -CH=), 7.55-7.6 (d, 1H, $J_{h,h}$ = 7.58 Hz, Trp -CH=), 7.6-7.7 (d, 1H, $J_{h,h}$ = 7.66 Hz, Trp -CH=), 7.6-7.9 (s, 1H, His -CH=), 8.0-8.1 (s, 2H, His -CH=).

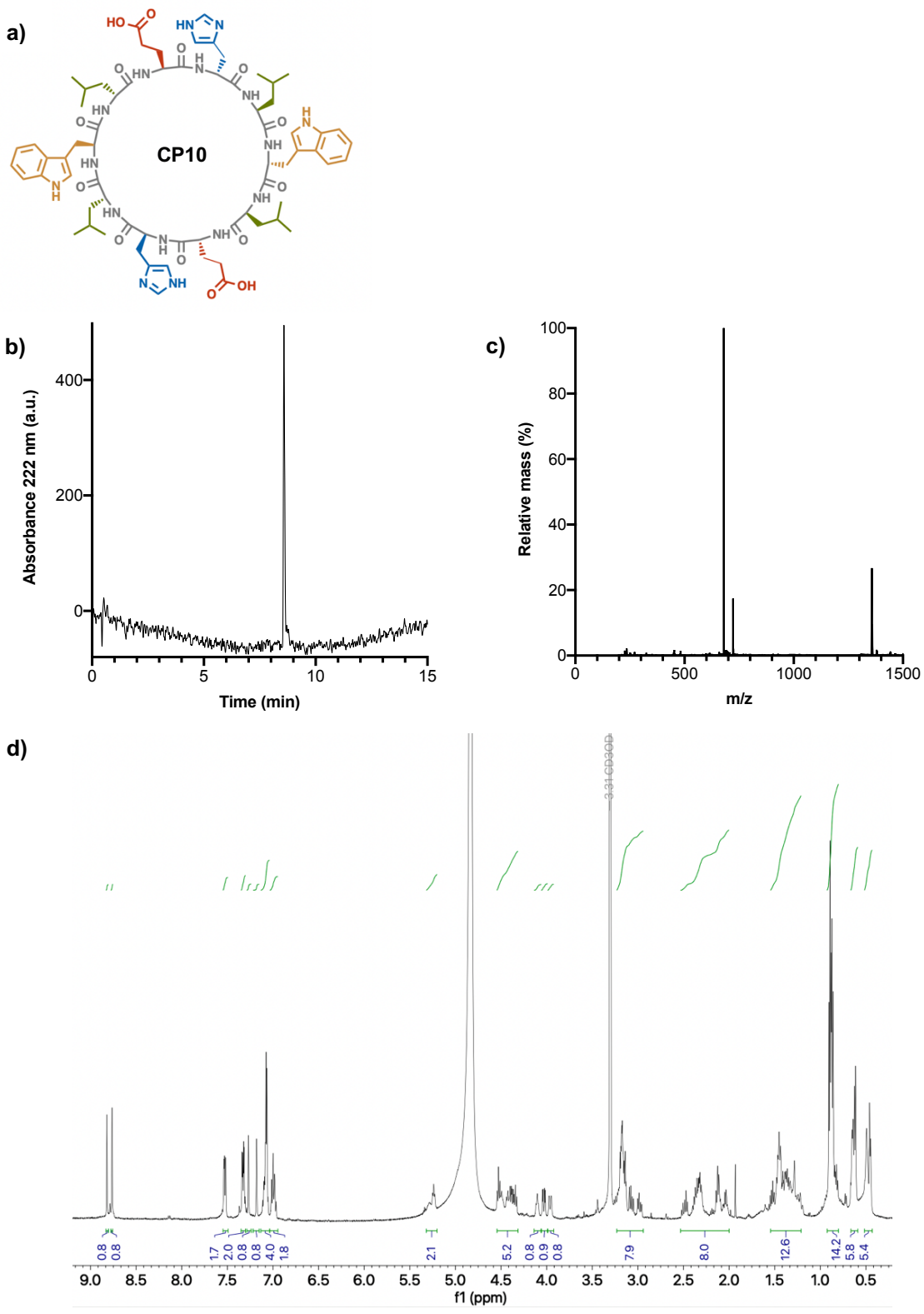

CP10 | *a) Molecular structure, b) Chromatogram after purification, c) MS spectrum from the main peak and d) ^{1}H-NMR (500 MHz) in CD_3OD.*

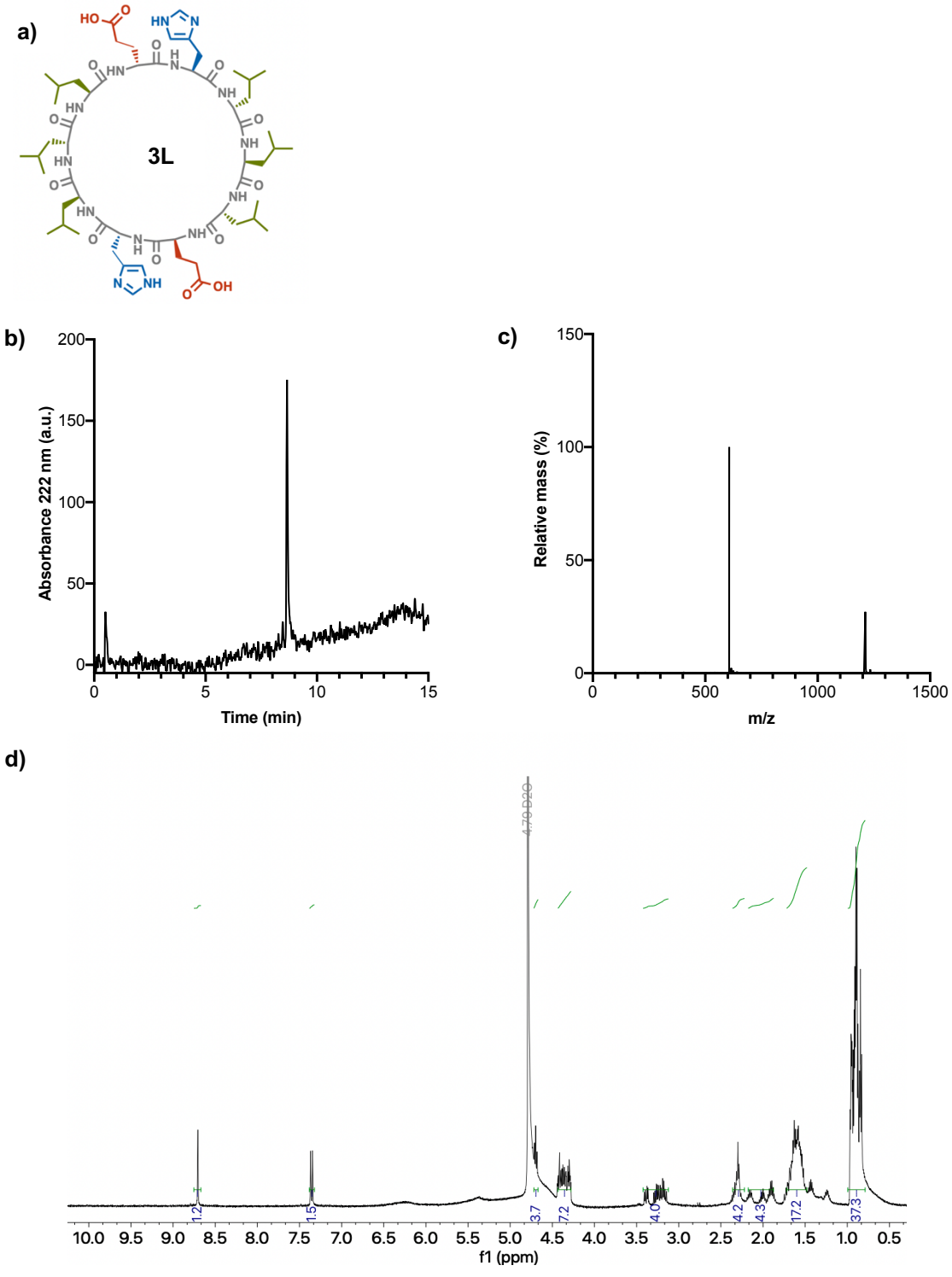

3L | *a) Molecular structure, b) Chromatogram after purification, c) MS spectrum from the main peak and d) ^{1}H-NMR (500 MHz) in D_2O.*

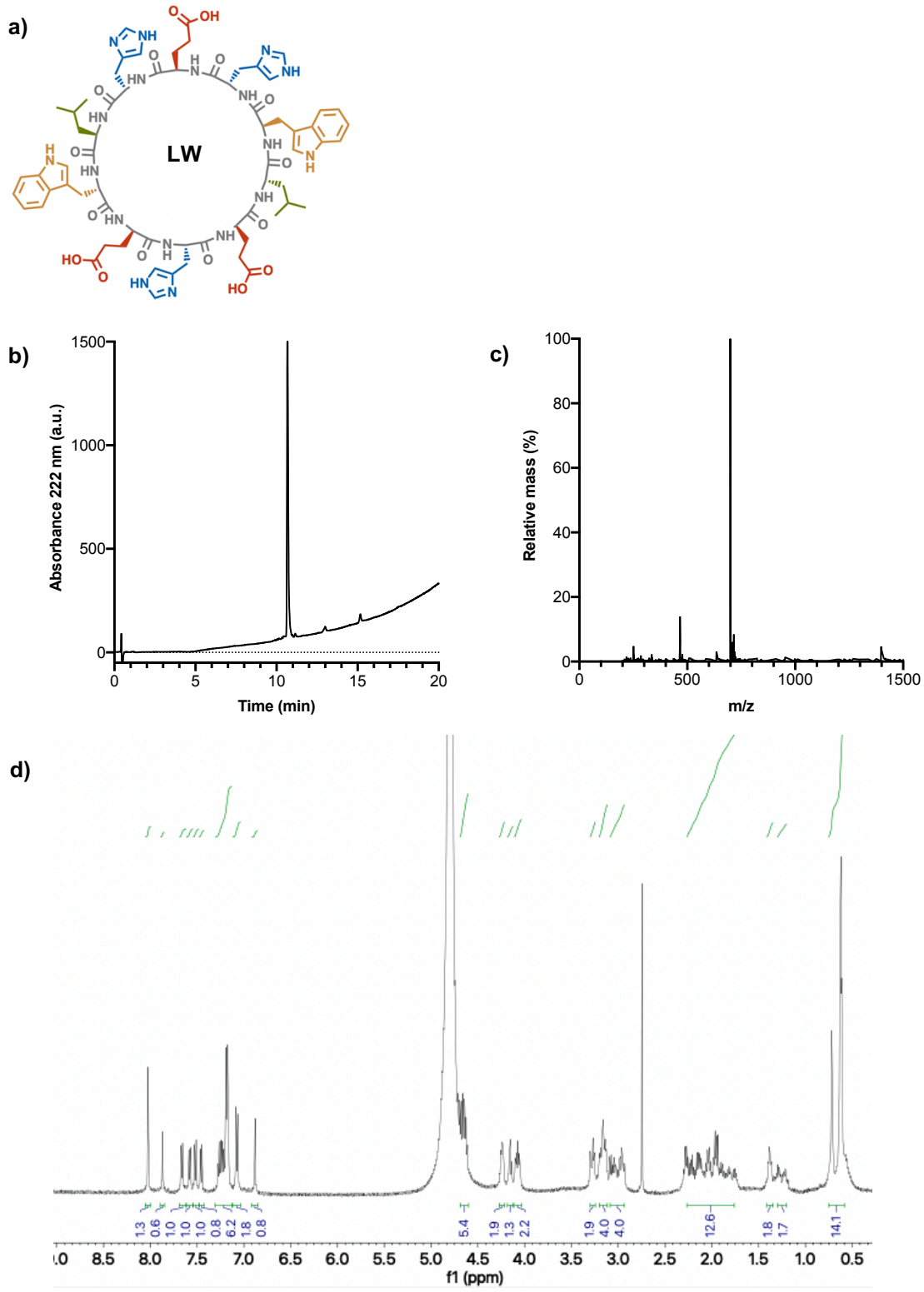

LW | *a) Molecular structure, b) Chromatogram after purification, c) MS spectrum from the main peak and d) ^{1}H-NMR (500 MHz) in D_2O.*

5. Methods

2D supramolecular assembly. A 100 μM solution of cyclic peptide (e.g. **CP10**) was prepared in 20 mM sodium phosphate buffer at pH 7.4. This sample was annealed by sequential sonication (5 min), heating (80°C/1.5 h/no shaking) and cooling (room temperature/1 h/no shaking) to assemble cyclic peptide monolayers. To explore assembly at other pH values, phosphate buffer was adjusted with HCl or NaOH before sonication, following the same protocol afterwards.

Epifluorescence microscopy. For epifluorescence, thioflavin-T was added to the cyclic peptide solutions to a final concentration of 10 μM before annealing. Then, nanosheets were assembled following the protocol above. 10 μL of the annealed sample were spotted on glass slides and left to dry completely at room temperature in the dark before imaging.

Scanning-transmission electron microscopy (STEM). Assembled peptide monolayers (see above) were diluted 10-fold with MilliQ water and 10 μL of the diluted sample were cast on TEM grids. After adsorption for 10 min, the excess solution was removed, and the sample was stained with phosphotungstic acid (1 $mg \cdot mL^{-1}$ in MilliQ water) for 1 min. Grids were then washed twice with MilliQ water (5 μL/1 min).

High-resolution transmission electron microscopy (HR-TEM). Assembled peptide monolayers (see above) were diluted 10-fold with MilliQ water and 10 μL of the diluted sample were cast on TEM grids. After adsorption for 10 min, the excess solution was removed, and grids were washed twice with MilliQ water (5 μL/1 min).

Atomic force microscopy (AFM). Assembled peptide monolayers (see above) were diluted 10-fold with MilliQ water and 10 μL of the diluted sample were cast on mica. After adsorption for 10 min, the excess solution was removed, and the mica surface was washed twice with MilliQ water. Image analysis was performed on Gwyddion.

Fourier-transform infrared spectroscopy (FT-IR). Assembled peptide monolayers (see above) were drop-cast directly on the diamond plate (ATR), left to dry, and FT-IR spectra were recorded at room temperature with subtracted background.

Circular dichroism (CD). Spectra were acquired at 25°C from a 2 mm-light path quartz cuvette, recording 60 accumulations between 390-190 nm at 200 $nm \cdot min^{-1}$, 2 s response time, 1 nm bandwidth, 0.2 nm data pitch. Data collected at a concentration of 100 μM for each peptide at pH 7.4 in phosphate buffer. Subtraction of the solvent background was done in all cases.

6. Modelling methods

All Atom (AA) model definition and Umbrella Sampling (US). We studied the stability of a single 8CP10-NT in aqueous solution via classical All Atom (AA) MD simulations carried out with the open-source software GROMACS 2016.6.[3] We compared two AA molecular models of 8CP10-NT including the CPs in parallel and antiparallel arrangement, respectively. Each single 8CP10-NT was first solvated in a box of 12.32x6.53x4.6 nm^3 with water molecules described by the tip3p model[4] and periodic boundary conditions applied in all box directions. The amber force field[5] was used to describe both bond and non-bonded interactions among CPs. Van der Waals and short-range electrostatic interactions were evaluated within a cut-off radius of 1.2 nm, while for the remaining long-range interactions, a particle-mesh Ewald summation[6] was applied to resolve electrostatics in the Fourier space. Our MD protocol consisted of a first step of energy minimisation and two consequent equilibration steps. Initially, to reach an equilibrium temperature of 298 K, we applied the canonical ensemble (NVT) for 100 ps using a Maxwell−Boltzmann speed distribution and the V-rescale thermostat[7] with a time constant = 0.1 ps. Subsequently, we set the isothermal-isobaric (NPT) ensemble for 1 ns at an equilibrium pressure of 1 bar and an equilibrium temperature of 298 K. In this step, we used the previous thermostat coupled with the Berendsen barostat[8] with a time constant of 2 ps. During the equilibration steps, the **CP10** atoms were restrained in their initial positions using a harmonic potential with a force constant of 1000 kJ/mol/nm^2. Once the desired thermodynamic conditions were reached, the restraint was removed and a 100 ns-MD run (integration step dt = 0.002 ps) was carried out by maintaining the temperature at 298 K with a Noose-hoover thermostat[9,10] (τ_T= 0.8 ps) and the pressure at p = 1 bar (τ_p= 2 ps) by imposing the Parrinello-Rahman barostat.[11] Along the MD simulation, the LINCS algorithm was employed to restrain the covalent bonds involving hydrogen atoms. To compare the stability of 8CP10-NT in parallel and antiparallel configuration, we analysed the production run trajectories by computing the interaction energy between the first two CPs within the nanotube, thereby including both Lennard-Jones and Coulomb potentials (see Figure 2).

The umbrella sampling (US) approach was used to calculate the potential of mean force (PMF) to bring two XCP10-NTs from a non-interacting distance to the assembled state, either in axial or lateral configuration. Note that the nanotubes (NTs) are denoted as XCP10-NTs, where 'X' indicates the oligomerisation degree (i.e. number of **CP10** units constituting the NT assembly). We compared the PMF obtained for two XCP10-NTs both in axial (with X ranging from 1 to 8) and lateral (with X ranging from 4 to 8) direction. A standard PMF profile is obtained, firstly, by placing two identical XCP10-NTs as close as possible to each other within a box sufficiently large to allow the movement of one XCP10-NT along the axial (or lateral) direction without being affected by the periodic imaging of the system; and secondly, by generating a total of forty US windows at increased centre of mass distances, "d", between the XCP10-NTs. Considering two consecutive windows, the XCP10-NTs have a displacement of 0.02 nm or 0.04 nm in the axial or later direction, respectively. Following the US protocol, for each US window we solvate the two XCP10-

NTs in explicit water (tip3p water model) and carried out two steps of equilibration, first in NVT and then in NPT ensemble, keeping the same parameters used in the equilibrium MD of 8CP10-NT previously described. A 10ns-MD-trajectory (integration step dt = 0.002 ps) was then carried out in NPT ensemble (Noose-hoover thermostat and Parrinello-Rahman barostat) by biasing the XCP10-NT position with a harming potential (spring constant of 50000 kJ/mol/nm^2). To obtain the PMF profiles, the XCP10v-NT reciprocal positions and forces were then extracted during the last 10 ns and processed using the weighted histogram analysis method[12] included in GROMACS 2020.2. Statistical errors of the PMF are estimated with bootstrap analysis.[13]

MetaDynamics (MetaD) simulation. To explore the free energy surface (FES) that represents the interaction between two 8CP10-NTs, we performed extensive 1μs-long Well-tempered Metadynamics (WT-MetaD) simulations.[14] We selected as collective variables (CVs) (i) the coordination number between the TRPs of the two 8CP10-NTs (R_0 = 0.5 nm) and (ii) the sum of the distances between the head and the tail CPs of the two NTs (Fig. 4A). In Figures 4A and S5, 'd_1' and 'd_2' represent the distance between the centre of mass of the two cyclic peptides at the top (green, d_1) and bottom (red, d_2) of two laterally-interfacing 8CP10-NTs (see cartoon in Fig. 4A). Note that the coordination number was computed as implemented in PLUMED 2.6.[15,16] These CVs were selected to represent unambiguously the orientation and the solvent exposure of the hydrophobic Trp residues. We chose a bias factor of 60, with an initial gaussian height of 1.5 kJ/mol, and a width of 0.1 nm and 10 nm for the distance and the coordination number, respectively. The gaussian deposition rate was set to 500 MD steps^{-1}, i.e. every 1 ps. After reaching convergence, we reweighted the FES using the Tiwary-Parrinello estimator[17] on the same CVs. All the WT-MetaD simulations were performed using GROMACS 2016.6[3] and PLUMED 2.6.[15,16]

Coarse-Grained (CG) model definition and CG self-assembly simulations. The Coarse-Grained (CG) model of one single cycle peptide (CP) was built by adopting the protein Martini force-field philosophy, which relies on an effective four-to-one mapping scheme.[18] In addition, virtual site dipoles were included into the CG-CP model to simulate the intermolecular backbone-backbone H-bonds between consecutive CPs. To reproduce the AA-CP trajectory within a stacked 1D nanotube, swarm-cg tool was then used to optimise all CG bond, angle, and dihedral parameters.[19]

CG self-assembly simulations of pre-stacked XCP10-NTs were carried out in an aqueous solution using a simulation box of 12x12x12 nm^3 filled with non-polarisable water particles, according to the Martini parametrisation. The number of counterions was adjusted to balance the charged XCP10-NTs. Our simulation protocol consisted of a 10 ns equilibration run to thermalise the system at p = 1 bar and T = 298 K; in this step, we used the velocity rescale[7] thermostat (τ_T= 1 ps) and Berendsen barostat[8] (τ_p= 8 ps). During the production runs, lasting 10 μs, we switched to the Parrinello−Rahman barostat,[11] still maintaining p = 1 bar and T = 298 K. A time-step of 10 fs was used to integrate Newton's equations of motion. Short-range interactions were truncated at 1.2 nm. Three-

dimensional periodic boundary conditions were applied. The simulations were performed using the open-source code GROMACS 2020.2.[3]

Estimation of the interfacial matching during NT dimerisation. A quantitative estimation of the interfacial matching can be derived by comparing both the orientation and position of two NTs while they are approaching and dimerising (Fig. S2A and Fig. S3A). We provide this quantitative evaluation in the case of dimerising 3CP10-NT (3mer) and 1CP10-NT (monomer), highlighting the enhancement in interfacial matching and consequentially the higher axial 2Delta G at higher NT oligomerisation.

In Fig. S2, we computed the angle (ϑ) between the two planes of dimerising cyclic peptide interfaces. The estimation of ϑ was carried out along the trajectory of a selected PMF window. When $\vartheta = 0$, and hence $\cos(\vartheta) = 1$, cyclic peptides are aligned, thereby showing a good propensity of interfacial matching. On the other hand, lower values of $\cos(\vartheta)$ indicate a misalignment between the NTs while they are approaching. The results in Fig. S2B clearly demonstrate that 1CP10-NT deviates from a reference orientation ($\cos(\vartheta) = 1$ of the blue profile) much more than 3CP10-NT (red curve). Therefore, shorter NTs are less favourable to match at the interface with an evident reduction in the axial dimerisation free energy (Delta G).

To provide a more robust and quantitative measurement of the interfacial matching, we also calculated the root mean square displacement between the dimerising cyclic peptide interfaces (Fig. S3). Fig. S3B confirms that 1CP10-NTs (green curve) are characterised during oligomerisation by a larger displacement (i.e. deviation) from an ideal position (deviation = 0 nm) than 3-mer NTs (red curve).

The quantitative estimate of interfacial matching reported in Figures S2 and S3 explains the increase in axial dimerisation free energy (axial ΔG) from short monomeric and dimeric species to larger 3-5mer CP10-NTs (Fig. 2D).

7. Supplementary figures

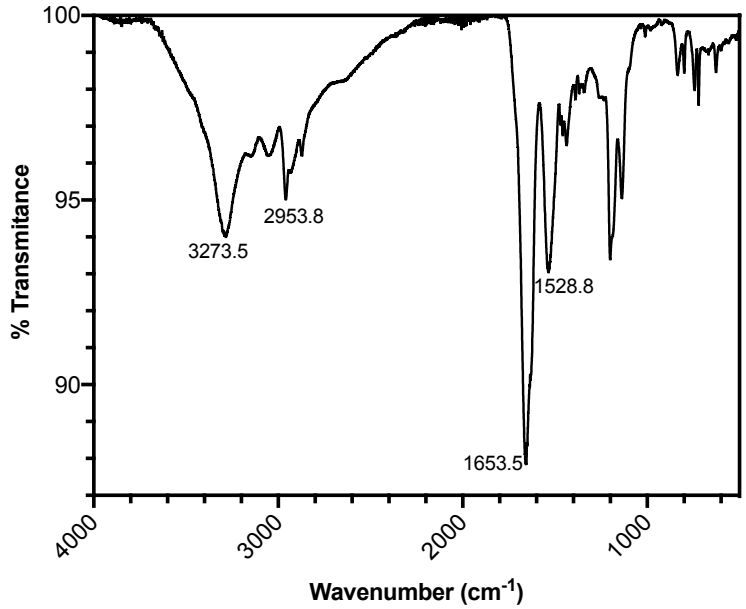

Figure S1 | *FT-IR spectrum of a freeze-dried sample of **CP10.** Peak labels of N-H stretching and amides I and II, respectively.*

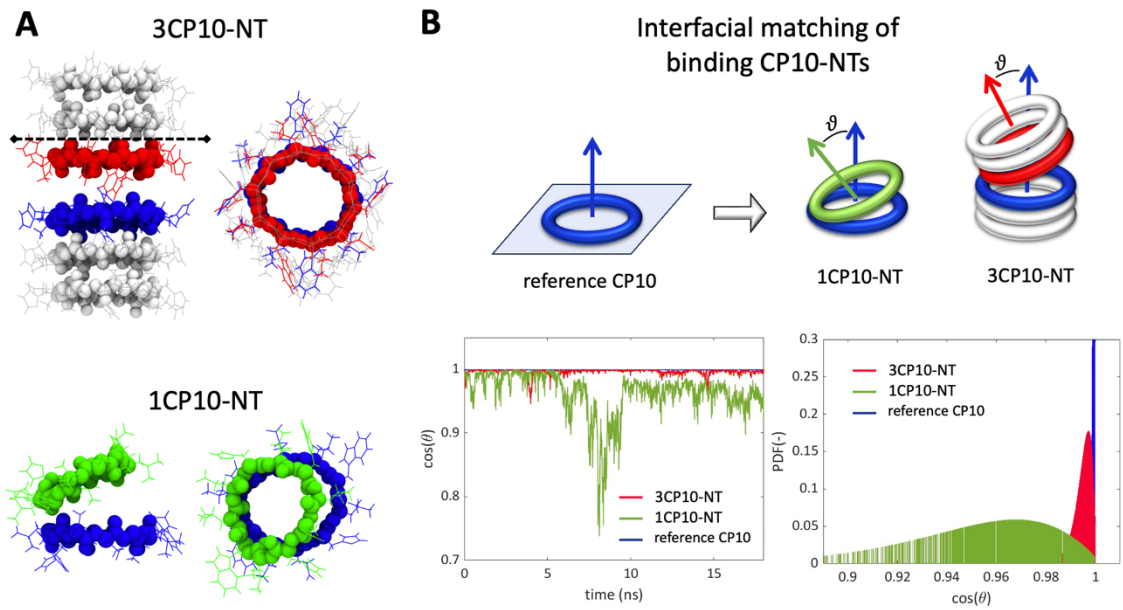

Figure S2 | *A) Side and front view of 3mer (3CP10-NT) and monomer (1CP10-NT) PMF snapshots at 0.7 nm distance during dimerisation. Blue cyclic peptides function as reference for red and green ones, which are selected to quantitatively estimate their interfacial matching. B) The interfacial matching of the NTs during the oligomerisation process is calculated from the angle (ϑ) between the plane of approaching NTs (green/red versus blue). The time distribution of cos(ϑ) and the probability distribution function (PDF) of cos(ϑ) show that the shorter 1CP10-NT interface deviates more from the ideal oligomerisation interface value of cos(ϑ) = 1.*

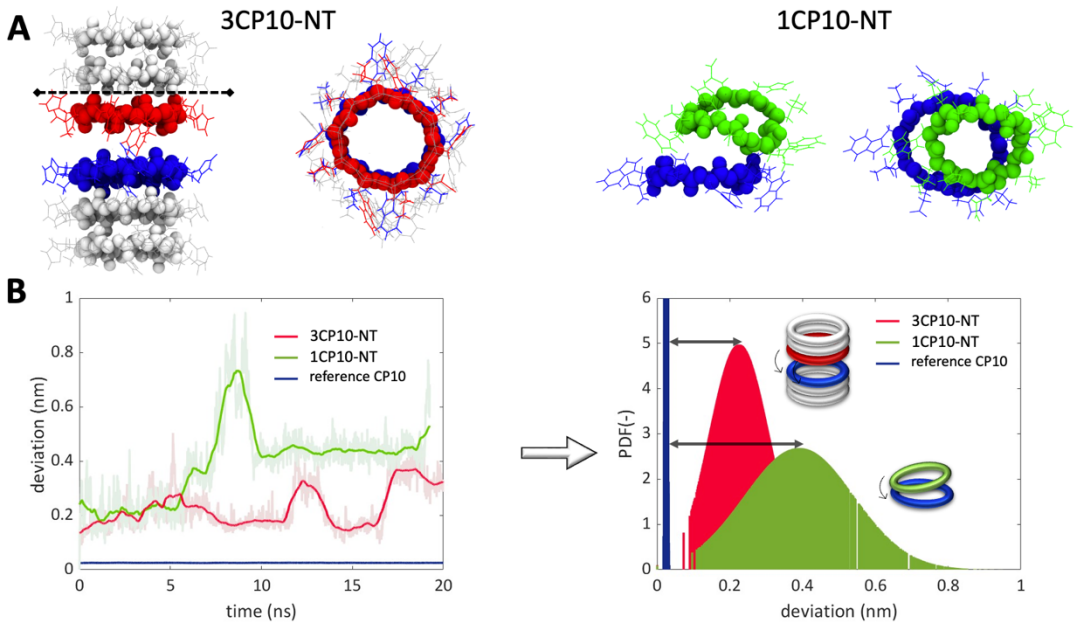

Figure S3 | *A) Side and front views of 3mer (3CP10-NT) and monomer (1CP10-NT) PMF snapshots at 0.7 nm distance during the dimerisation. Blue cyclic peptides function as reference for red and green ones, which are selected to compute the deviation from the reference cyclic peptide position and hence give a quantitative measurement of the interfacial matching. B) Left: Deviation over time between the red (3CP10-NT) and green (1CP10-NT) cyclic peptide interfaces with a reference one (blue), which is computed as the root means square displacement. The probability distribution function (PDF) of the deviation shows that the shorter 1CP10-NT deviates more from its reference while the oligomerisation takes place (PMF).*

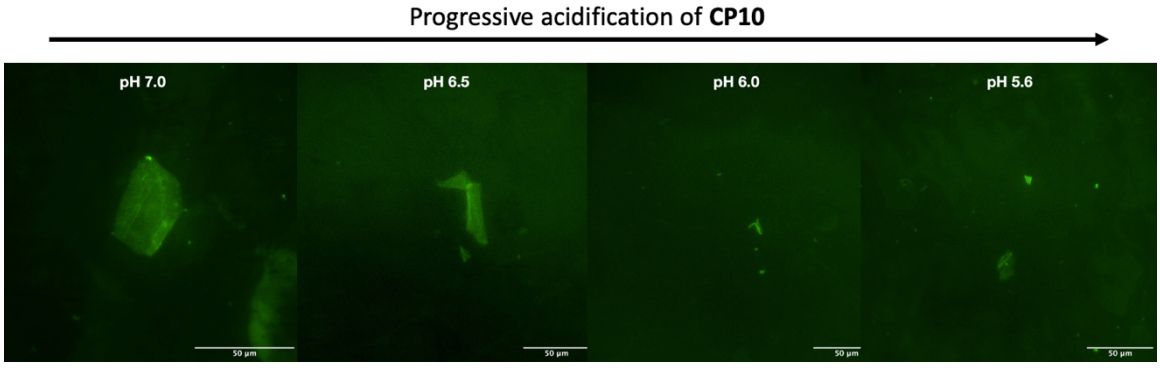

Figure S4 | *Epifluorescence micrographs of **CP10** 2D monolayers prepared at different pH values (see Methods). Samples stained with Thioflavin-T. All scale bars = 50 µm.*

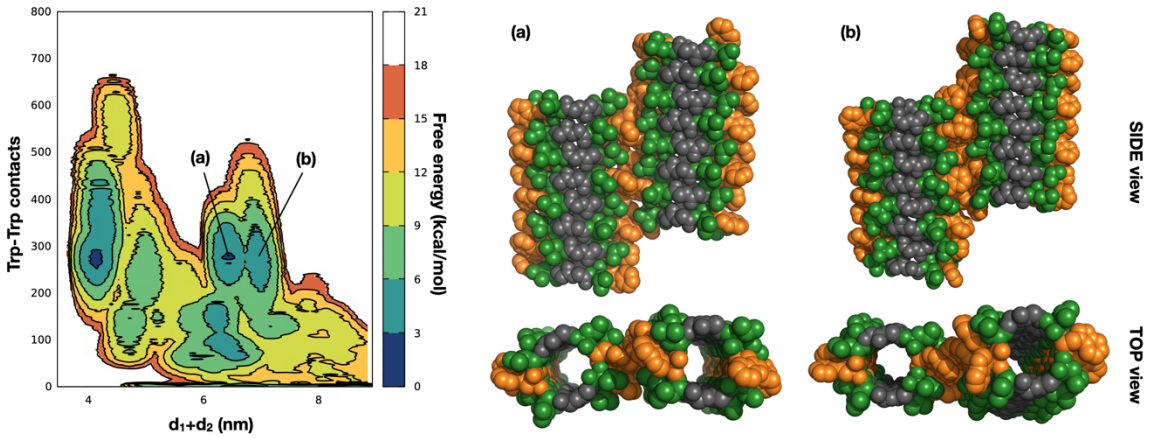

Figure S5 | *Representative structures of two 8CP10-NTs in free energy surface metadynamics simulation with values of $d_1+d_2 > 5$ (expansion of Fig. 4A). Trp and Leu residues are coloured in orange and green, respectively.*

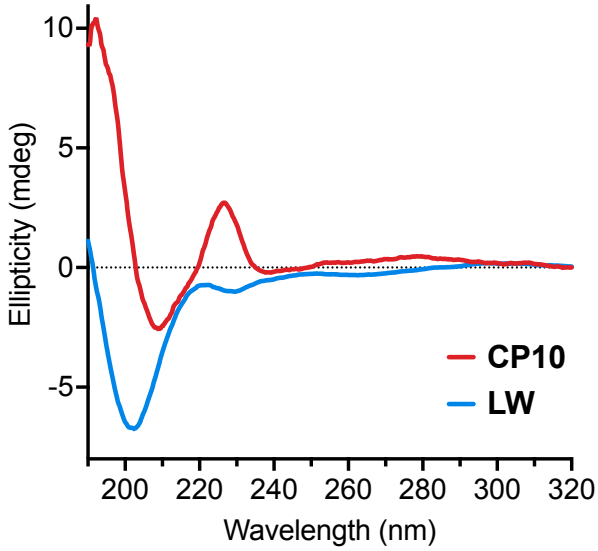

Figure S6 | *Circular dichroism (CD) spectra of annealed samples of **CP10** and **LW**.*

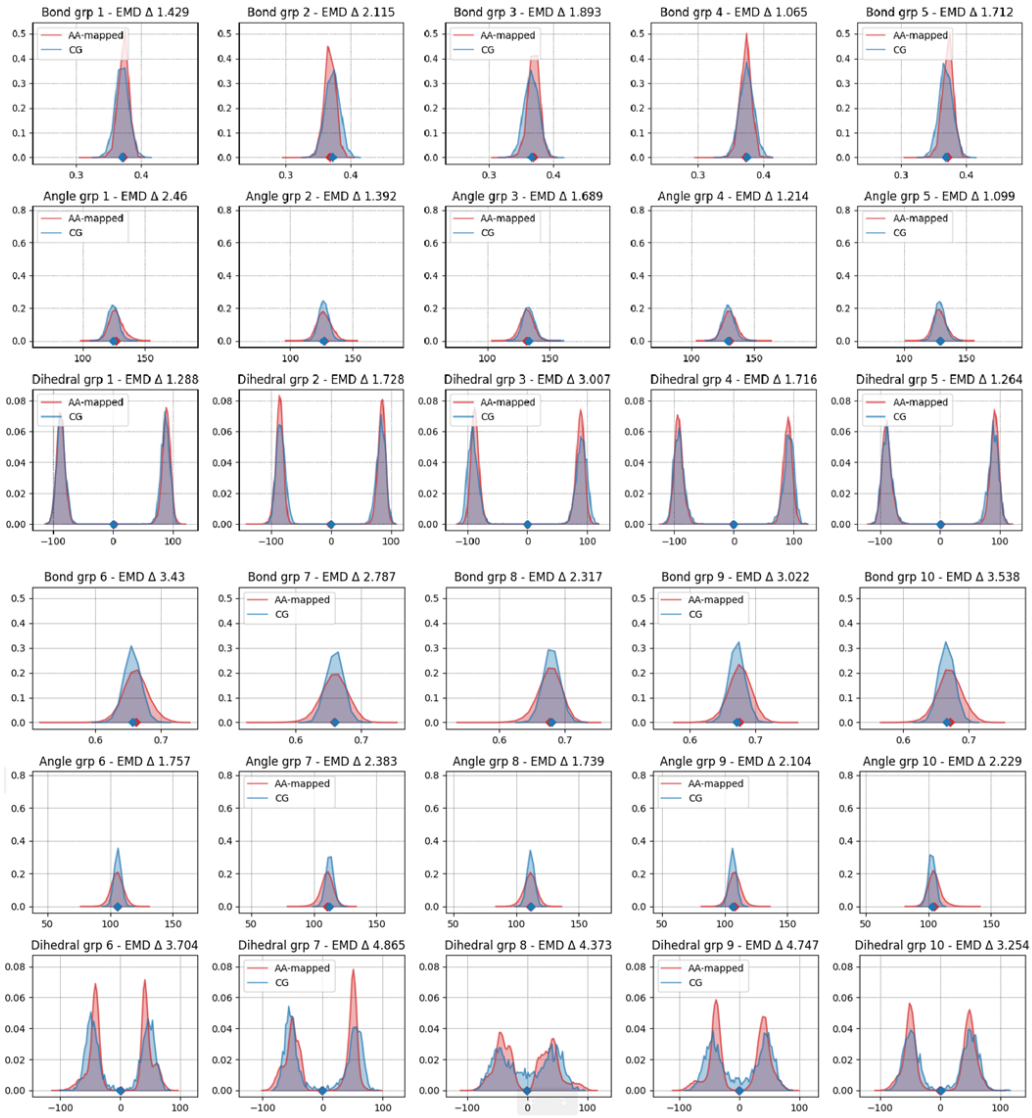

Figure S7 | *Validation of the bond and angle distributions in a single Cyclic Peptide simulated in both all-atom (AA) and coarse-grained (CG) models by using SwarmCG. The itp file with the AA vs CG bead mapping is available in the repository link reported in the DATA AVAILABILITY section of the manuscript.*

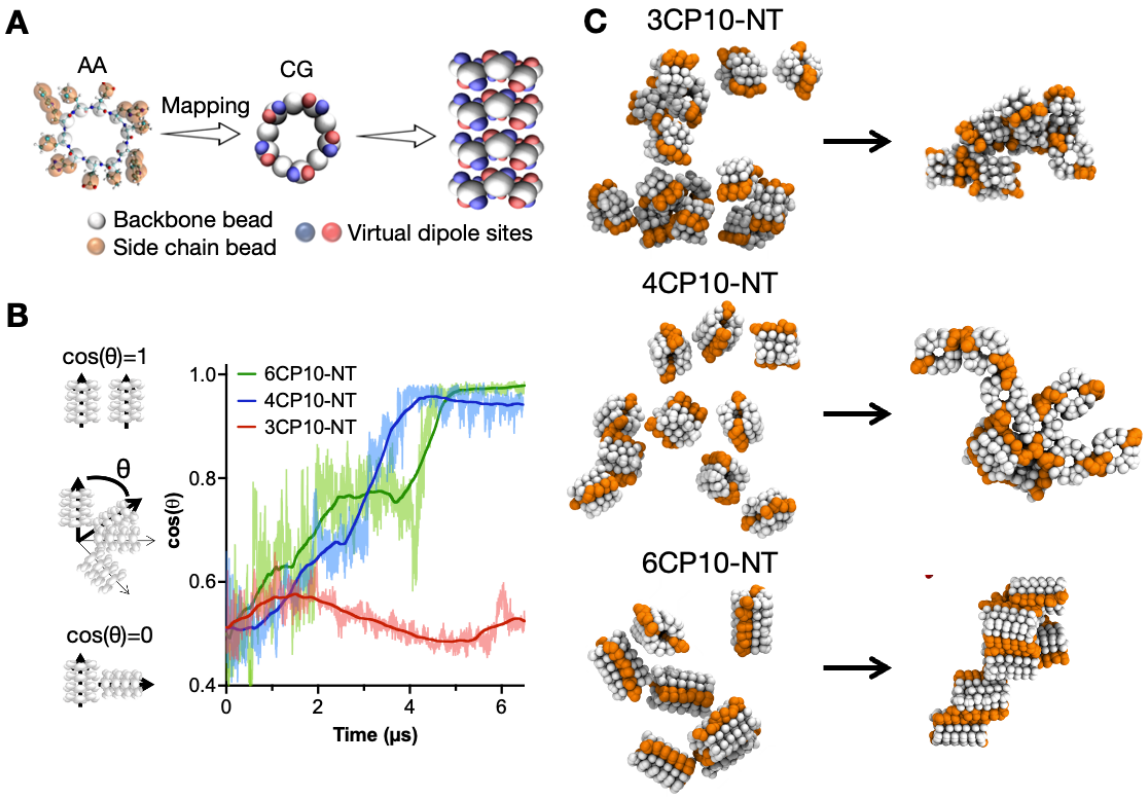

Figure S8 | *(A) Coarse-grained (CG) mapping of all-atoms (AA)* ***CP10*** *structure and nanotube (NT) assembly. (B) Time evolution of the average cos(θ) between the tube central axes of all possible NT pairs. Randomly oriented NTs generate a cos(θ) = 0.5 at the beginning of the simulation, which can evolve over time to an all-parallel configuration (i.e. cos(θ) = 1). (C) Examples of CG-MD snapshots of CP10-NTs of different 1D oligomerisation states (3, 4 and 6) in aqueous solution. The snapshots show the CP10-NT configurations at the initial state (left) and after 5 μs of CG-MD simulations (right). Orange beads indicate hydrophobic tryptophan residues working as 2D propagation interfaces.*

8. Supplementary references

(1) A. Méndez-Ardoy, I. Insua, J. R. Granja and J. Montenegro, 2022, vol. 2371, pp. 449–466.

(2) C. Kay, O. E. Lorthioir, N. J. Parr, M. Congreve, S. C. McKeown, J. J. Scicinski and S. V. Ley, *Biotechnol. Bioeng.*, 2000, **71**, 110–118.

(3) M. J. Abraham, T. Murtola, R. Schulz, S. Páll, J. C. Smith, B. Hess and E. Lindahl, *Softwarex*, 2015, **1**, 19–25.

(4) D. J. Price and C. L. Brooks, *J. Chem. Phys.*, 2004, **121**, 10096–10103.

(5) K. Lindorff-Larsen, S. Piana, K. Palmo, P. Maragakis, J. L. Klepeis, R. O. Dror and D. E. Shaw, *Proteins: Struct. Funct. Bioinform.*, 2010, **78**, 1950–1958.

(6) T. Darden, D. York and L. Pedersen, *J. Chem. Phys.*, 1993, **98**, 10089–10092.

(7) G. Bussi, D. Donadio and M. Parrinello, *J. Chem. Phys.*, 2007, **126**, 014101.

(8) H. J. C. Berendsen, J. P. M. Postma, W. F. van Gunsteren, A. DiNola and J. R. Haak, *J. Chem. Phys.*, 1984, **81**, 3684–3690.

(9) S. Nosé, *Mol. Phys.*, 1984, **52**, 255–268.

(10) W. G. Hoover, *Phys. Rev. A*, 1985, **31**, 1695–1697.

(11) M. Parrinello and A. Rahman, *J. Appl. Phys.*, 1981, **52**, 7182–7190.

(12) M. Souaille and B. Roux, *Comput. Phys. Commun.*, 2001, **135**, 40–57.

(13) J. S. Hub, B. L. de Groot and D. van der Spoel, *J. Chem. Theory Comput.*, 2010, **6**, 3713–3720.

(14) A. Barducci, G. Bussi and M. Parrinello, *Phys. Rev. Lett.*, 2007, **100**, 020603.

(15) G. A. Tribello, M. Bonomi, D. Branduardi, C. Camilloni and G. Bussi, *Comput. Phys. Commun.*, 2014, **185**, 604–613.

(16) M. Bonomi, G. Bussi, C. Camilloni, G. A. Tribello, P. Banáš, A. Barducci, M. Bernetti, P. G. Bolhuis, S. Bottaro, D. Branduardi, R. Capelli, P. Carloni, M. Ceriotti, A. Cesari, H. Chen, W. Chen, F. Colizzi, S. De, M. D. L. Pierre, D. Donadio, V. Drobot, B. Ensing, A. L. Ferguson, M. Filizola, J. S. Fraser, H. Fu, P. Gasparotto, F. L. Gervasio, F. Giberti, A. Gil-Ley, T. Giorgino, G. T. Heller, G. M. Hocky, M. Iannuzzi, M. Invernizzi, K. E. Jelfs, A. Jussupow, E. Kirilin, A. Laio, V. Limongelli, K. Lindorff-Larsen, T. Löhr, F. Marinelli, L. Martin-Samos, M. Masetti, R. Meyer, A. Michaelides, C. Molteni, T. Morishita, M. Nava, C. Paissoni, E. Papaleo, M. Parrinello, J. Pfaendtner, P. Piaggi, G. Piccini, A. Pietropaolo, F. Pietrucci, S. Pipolo, D. Provasi, D. Quigley, P. Raiteri, S. Raniolo, J. Rydzewski, M. Salvalaglio, G. C. Sosso, V. Spiwok, J. Šponer, D. W. H. Swenson, P. Tiwary, O. Valsson, M. Vendruscolo, G. A. Voth and A. White, *Nat. Methods*, 2019, **16**, 670–673.

(17) P. Tiwary and M. Parrinello, *J. Phys. Chem. B*, 2015, **119**, 736–742.

(18) L. Monticelli, S. K. Kandasamy, X. Periole, R. G. Larson, D. P. Tieleman and S.-J. Marrink, *J. Chem. Theory Comput.*, 2008, **4**, 819–834.

(19) C. Empereur-Mot, L. Pesce, G. Doni, D. Bochicchio, R. Capelli, C. Perego and G. M. Pavan, *ACS Omega*, 2020, **5**, 32823–32843.